Heliyon 10 (2024) e38181

Contents lists available at ScienceDirect

Heliyon

journal homepage: www.cell.com/heliyon

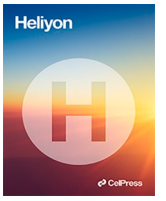

Research article

Quercetin activates autophagy in the distal ischemic area of random skin flaps through Beclin1 to enhance the adaptability to energy deficiency

Xin Zheng [a,1], Yiyu Wang [b,1], Xiaokang Gong [a,1], Weijie Chen [a], Wenbiao Zheng [a,**], Tao Chen [a,*]

[a] Department of Orthopedics, Municipal Hospital Affiliated to Taizhou University, Zhejiang, Taizhou, 318000, China
[b] Zhejiang Provincial Key Laboratory of Plant Evolutionary Ecology and Conservation, Taizhou Key Laboratory of Biomedicine and Advanced Dosage Forms, School of Life Sciences, Taizhou University, Zhejiang Taizhou, 318000, China

ARTICLE INFO

Keywords:
Random flaps
Quercetin
Autophagy
Angiogenesis
ERK

ABSTRACT

Random flaps are frequently employed in treating substantial skin abnormalities and in surgical tissue-rebuilding interventions. The random flap technique provides flaps of specific dimensions and contours to fit the surgical incision. However, blood supply deficiency and subsequent ischemia-reperfusion injury can cause severe oxidative stress and apoptosis, eventually leading to distal necrosis, which limits the clinical application of the flap. Quercetin (QUE) is primarily found in the glycoside form in many plant parts, such as stem bark, flowers, leaves, buds, seeds, and fruits. Cellular, animal, and clinical studies have demonstrated the antioxidant, anti-apoptosis, anti-inflammatory, and activation of autophagy properties of QUE. In previous studies, high doses of QUE effectively suppressed the survival of human umbilical vein endothelial cells (HUVECs) stimulated by hydrogen peroxide. However, different concentration gradients of QUE on HUVECs revealed a significant protective effect at a concentration of 10 mM. The protective impact of QUE on HUVECs was evaluated using scratch tests, CCK-8 assays, and EDU assays. Simultaneously, a mouse model of random skin flap was created, and the impact of QUE on skin flap survival was examined by intragastric injection. The QUE group showed a significantly larger survival area of the random flap and higher blood flow intensity compared to the control group. Furthermore, the beneficial effects of QUE were reversed by the autophagy inhibitor 3-MA. Therefore, autophagy plays a significant role in the therapeutic benefits of QUE on flap survival.

1. Introduction

A skin flap consists of skin, blood supply, and the attached subcutaneous adipose tissue [1]. Flap transplantation technology is widely used in skin defects and plastic surgery [2]. The random flap is not centered on a specific vessel and has its blood supply from the microvascular network at its pedicle [3,4]. Therefore, the random flap can be used on almost any body surface. However, distal

* Corresponding author. Department of Orthopedics, Municipal Hospital Affiliated to Taizhou University, Zhejiang, Taizhou, 318000, China.
** Corresponding author. Department of Orthopedics, Municipal Hospital Affiliated to Taizhou University, Zhejiang, Taizhou, 318000, China.
E-mail addresses: Zwbspine@163.com (W. Zheng), slyy_01066@tzc.edu.cn (T. Chen).
[1] Xin Zheng, Yiyu Wang and Xiaokang Gong contributed equally to this work.

https://doi.org/10.1016/j.heliyon.2024.e38181
Received 15 April 2024; Received in revised form 19 September 2024; Accepted 19 September 2024
Available online 29 September 2024
2405-8440/© 2024 Published by Elsevier Ltd. This is an open access article under the CC BY-NC-ND license (http://creativecommons.org/licenses/by-nc-nd/4.0/).

tissue ischemia is more prevalent due to the lack of axial blood vessels [5]. In addition, neovascularization leads to blood reperfusion, and oxidative stress and apoptosis during blood reperfusion decreases the survival of the flap after transplantation [6–10].

Autophagy is a widely preserved mechanism in eukaryotic cells for recycling macromolecules and depends on lysosomes [11–13]. Cellular contents, such as damaged proteins and organelles, are engulfed and autophagy provides cells with the nutrients and materials needed for self-renewa [14–16]. However, autophagy has been described as a "double-edged sword." The role of autophagy also varies across different types of flaps: it plays a positive role in random flaps but a negative role in perforator flaps [17–21]. This disparity might be attributed to the different pathways that activate autophagy and the degree of activation. Autophagy plays an active and crucial role in various ischemia-hypoxia and ischemia-reperfusion models, contributes to angiogenesis, reduces oxidative stress, and attenuates apoptosis, such as in HUVECs stimulated by hydrogen peroxide [22–28].

QUE is widely found in vegetables, fruits, and other common plant foods [29–31]. Cell, animal, and clinical studies have demonstrated its anti-oxidative, anti-apoptosis, and anti-inflammatory properties [32–35]; moreover, QUE has been confirmed to act on the Beclin1 signaling pathway to affect autophagy [36–38]. Nevertheless, the literature does not currently provide any reports on whether QUE can govern the survival of random skin flaps by autophagy. This work aimed to investigate the QUE impact on the viability of mouse voluntary skin flaps and to examine the potential of activating the autophagy process through the Beclin1 signaling pathway to promote the survival area of a random flap.

2. Materials and methods

2.1. Reagents

The reagent used in this study was quercitrin (C21H20O11; purity≥98 %), which was obtained from Meilun Biotech (Dalian, China). The compound 3-methyladenine (3 MA; C6H7N5; purity≥98 %) was acquired from Sigma-Aldrich Chemical Company (Milwaukee, WI, United States).

2.2. Cell culture

HUVECs were obtained from the Chinese Academy of Sciences (Shanghai, China). The cells were cultured in DMEM enriched with 10 % FBS and 1 % penicillin/streptomycin. The cells were incubated at 37 °C and 5 % CO_2. The cells were consistently monitored. The culture medium was periodically refreshed every 2–3 days, and the cells in the logarithmic growth phase were preferentially enriched for further experimental procedures.

2.3. Drug administration in cell

Control group: nothing is done to the cells.
QUE group: add 90 μM QUE.
QUE+3 MA group: add 90 μM QUE5 and mM 3 MA.
QUE + Compound C group: add 90 μM QUE and 1 μM Compound C.
MK8722 group: add 100 nM MK8722.

2.4. Drug administration in animal

The mice in the QUE and QUE+3 MA groups received intraperitoneal injection of QUE at a dose of 10 mg/kg/d for 7 days [39], while the control group received an equal amount of physiological saline. After intraperitoneal injection of 3 MA (15 mg/kg/d) for 30 min [40], SIN was injected again.

2.5. Wound healing assay

The wound healing experiment was performed to determine the migratory capacity of HUVECs. Concisely, the cells were inoculated into 6-well plates at a density of 1×10^5 cells per well. After reaching complete confluence, the cellular monolayer was mechanically subjected to a process resulting in the creation of a "wound". The wound area was measured using ImageJ software (NIH, Bethesda, MD, United States) and the migration rate of cells was calculated at time intervals of 0, 6, 12, and 24 h.

2.6. BrdU assay

First, HUVECs were pre-exposed to QUE at a concentration of 10uM for 24h, exposed to hydrogen peroxide at a concentration of 1.9 mM for 24h, and introduced into a serum-free basic medium. The 20uM BrdU working solution was prepared by combining the basic medium with the previous cell culture solution for co-culture for 2–6h. The subsequent steps strictly followed the kit instructions. Cell proliferation was analyzed using images randomly selected from a Nikon fluorescence microscope, and the results were calculated.

2.7. Transwell assay

Cell migration ability was assessed by employing the transwell assay. Following trypsinization with 0.25 % trypsin, the HUVECs were centrifuged, resuspended, and then seeded into 24-well plates. In the experimental procedure, 50,000 cells were placed in the upper chamber (Corning, Beijing, China). Concurrently, a volume of 400 μL of DMEM enriched with 10 % FBS was introduced into the lower chamber. The cells were then incubated for 24 h at a temperature of 37 °C, and the upper chamber was gently wiped using cotton swabs to eliminate cells that did not migrate. The cells were fixed with 4 % paraformaldehyde for 10 min prior to staining with 0.5 % crystal violet. The cells were then rinsed with flowing water and a microscope was used to count the number of cells. The experiment was independently conducted three times.

2.8. Cell counting kit-8 (CCK-8) assay

The CCK-8 assay was employed to assess the proliferative activity of HUVECs. The cells were collected during the logarithmic growth phase to create a suspension of cells. Once the suspension of cells was ascertained, the cells were introduced onto 96 well plates at a density of 1×10^3 cells per well, with three duplicates for each group. Subsequently, the cells were subjected to a 24-h incubation period in accordance with the provided instructions. A 10 μl volume of CCK8 reagent (Dojindo Molecular Technologies in Kumamoto, Japan) was introduced into each well, and the cells were incubated at 37 °C for 1 h. Finally, the absorbance at 450 nm wavelength (OD value) of each well was measured with a microplate reader.

2.9. Animal model of random skin flap

A total of ninety C57BL/6 mice (male, weighing between 22 and 25 g) were procured from the Experimental Animal Center of Tai Zhou University(authorization number: TZXY-2023-20231055). The Animal Care and Use Committee at Tai Zhou University granted ethical approval for the animal trials. The mice were randomly assigned to three groups, namely a control group, a treatment group receiving QUE, and a treatment group receiving QUE +3 MA. Prior to the surgical procedure, the mice were subjected to anesthesia using a 1 % solution of sodium pentobarbital (50 mg/kg, IP). The mouse dorsal random flap model, measuring 4×1.5 cm^2, was set up on the central dorsal region. Subsequently, the arteries supplying the flap were entirely severed. Ultimately, the detached flap was fastened employing a 4-0 silk suture. The flap was divided into three regions based on their proximity to the flap pedicle: distal (area I), intermediate (area II), and proximal (area III) zones. The mice were euthanized on postoperative day 7 (POD 7), and flap tissues were collected for further experimental analysis.

2.10. Laser Doppler perfusion image

Laser Doppler Blood Flow (LDBF) imaging was utilized to evaluate the blood supply and vascular flow of the flap, thereby assessing angiogenesis. Mice were placed in a prone position within the scanning area while under narcosis. The laser Doppler imager was utilized to scan the whole flap area, and color-coded live body flow images were obtained on postoperative days 0, 3, and 7. The blood flow was quantified in perfusion units using moorLDI Review software (version 6.1). The scanning and analysis of all mice were conducted three times, and the mean value was computed for additional statistical evaluation.

2.11. Flap survival evaluation

Following anesthesia, high-resolution images of the dorsal skin flap were captured by a digital camera on the third and seventh postoperative days (PODs). The survival and ischemic regions were assessed utilizing Image-Pro Plus imaging software (version 6.0; Media Cybemetics). The survival area was quantified as a percentage by multiplying the computed value by 100 %.

2.12. Hematoxylin and eosin (H&E) staining and masson staining

The mice were euthanized using an overdose of pentobarbital sodium (Solarbio Science & Technology, Beijing, China) after 7 days. A total of six tissue samples were surgically removed from the central region of the second choke vessel zone (SCV) in every experimental group, measuring 0.5 cm × 0.5 cm in size. These samples were then post-fixed in a 4 % (v/v) paraformaldehyde solution for a duration of 24 h and embedded in paraffin wax. Subsequently, the samples were sliced into sections of 4 μm in thickness and subjected to staining with H&E using established histology techniques (Solarbio Science & Technology, Beijing, China). A total of six fields were chosen at random from three distinct sections to observe angiogenesis using a light microscope (Olympus Corp, Tokyo, Japan). Furthermore, the microvascular density (MVD) was quantified by calculating the number of microvessels per unit area/mm^2.

2.13. Immunofluorescence

A total of six specimens underwent deparaffinization and rehydration, following the established protocol for IHC. A solution of hydrogen peroxide with a concentration of 3 % (v/v) was employed, and tissue antigen retrieval was conducted using a sodium citrate buffer with a concentration of 10.2 mM. In addition, a solution of 0.1 % (v/v) PBS-Triton X-100 was applied to the samples to facilitate permeation. The slides were blocked using 10 % (v/v) normal goat serum for a duration of 1 h and then incubated overnight at a

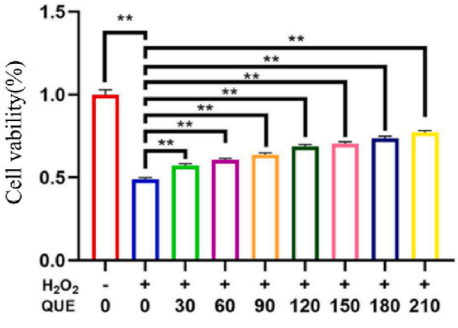

(a)

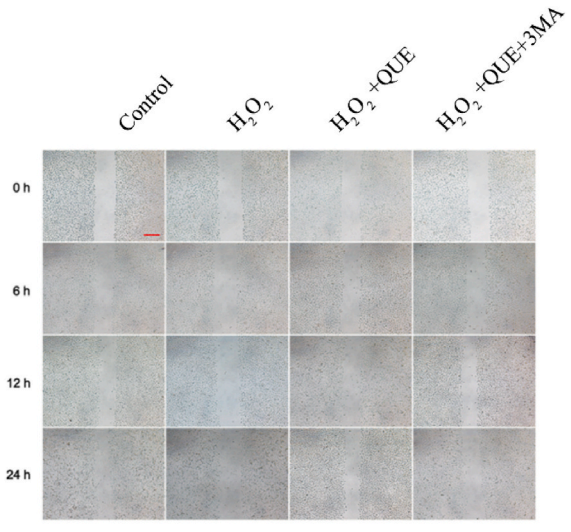

(b)

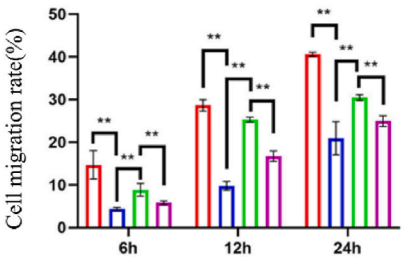

(c)

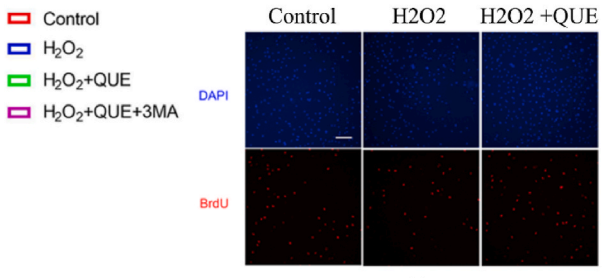

(d)

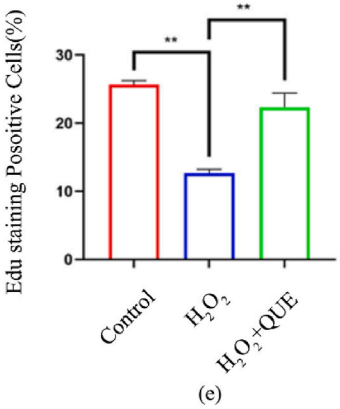

(e)

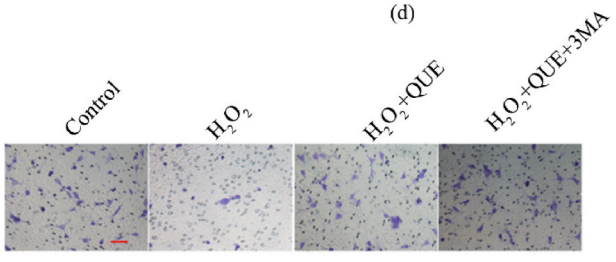

(f)

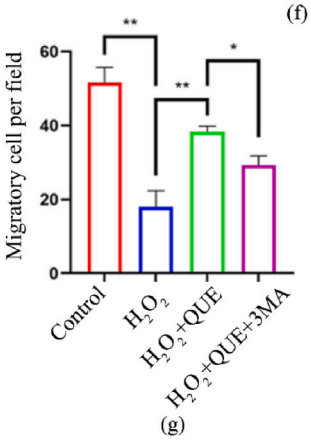

(g)

(caption on next page)

Fig. 1. |**QUE enhanced the proliferation and migration of HUVECs following oxidative stress injury**. (a) Cell viability of each cell. (b) Images of wound healing in the control, H_2O_2, H_2O_2+QUE and H_2O_2+QUE+3 MA groups. Images were captured at 0, 6, 12, and 24 h after the scratch. Magnification: 4×; scale: 400 μm. (c) Cell migration rate that were affected by the abovementioned factors for 6, 12, and 24 h (d) BrdU assay reveals the proliferation status of different groups of cells. Magnification: 10×; scale: 200 μm. (e) The statistical analysis of Edu-stained positive cells in the control group, H_2O_2 group, and H_2O_2+QUE group. (f) transwell assay demonstrates the migratory capacity of cells in different groups.(g)Migratory cell per field. Data were expressed as mean ± SD, n = 3. "*"and"**" represent $p < 0.05$ or $p < 0.01$ versus the H_2O_2 and QUE groups, indicating statistical significance. Magnification: 20×; scale: 100 μm.

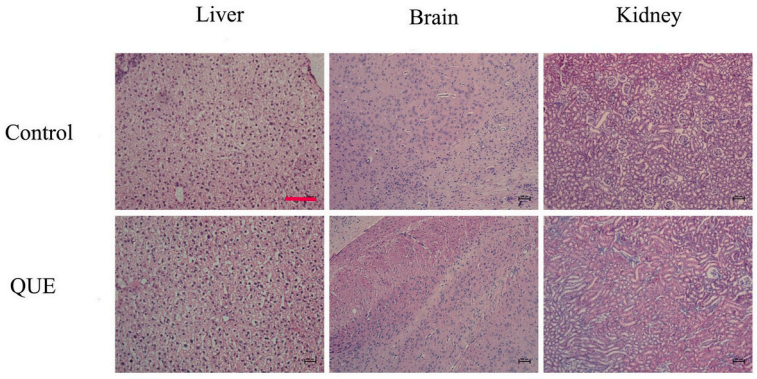

(a)

EXAMINE	CONTROL	CIONTROL+HES	REFERENCE RANGE
CRE	22±5	19±8	11-28
ALT	36±7	32±6	13-43
AST	48±9	59±11	12-89

(b)

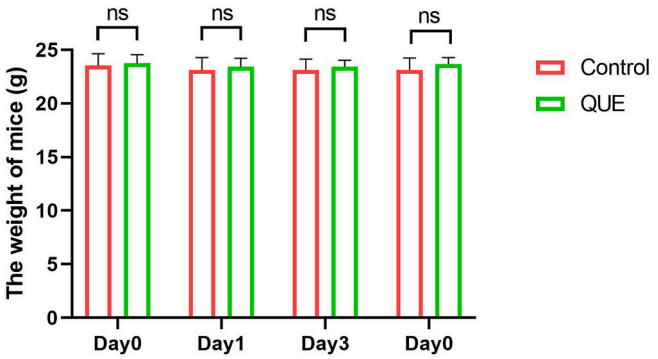

(c)

Fig. 2. |**Systemic administration of QUE does not cause significant toxic damage**. (a) H and E staining of the brain, kidneys, and spleen of mice in each group. Magnification: 10×; Scale bar 200 μm. (b) Blood biochemical test in each group. Data were expressed as mean ± SD, n = 3. n.s. represents no statistical significance.

temperature of 4 °C with primary antibodies targeting C-CASP3 (dilution of 1:200, CST, USA), CD34 (dilution of 1:200, Abcam, UK), LC3II (dilution of 1:200, Sigma, Milwaukee, USA), and P62 (dilution of 1:200, Proteintech, USA). Subsequently, the specimens were incubated with the corresponding secondary antibodies at ambient temperature for 1 h. Additionally, the nuclei were stained using DAPI (Beyotime Biotechnology, Jiangsu, China). All photographs were evaluated using a fluorescence microscope (Olympus, Tokyo,

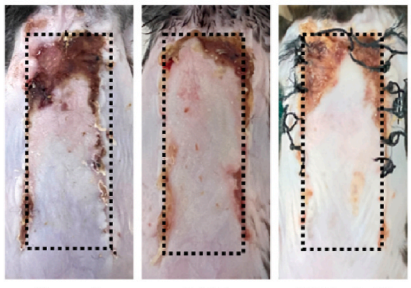

(a)

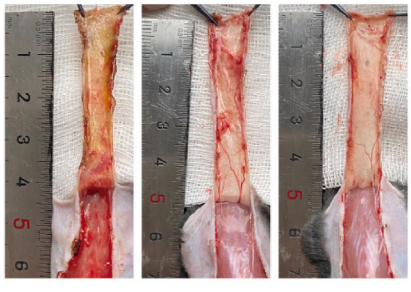

(c)

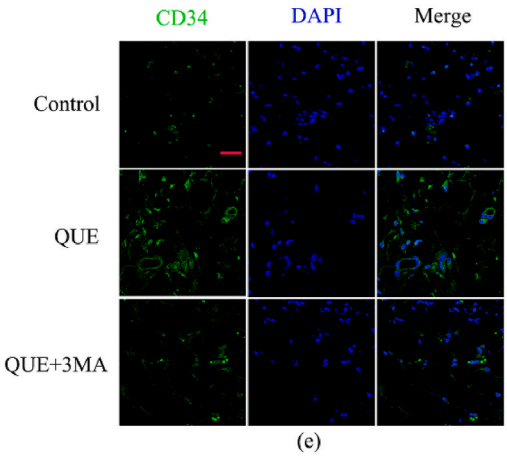

(e)

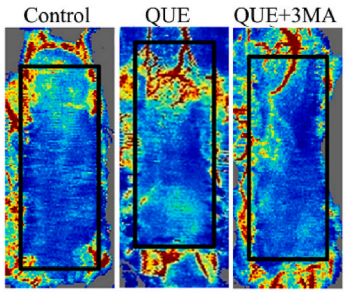

(g)

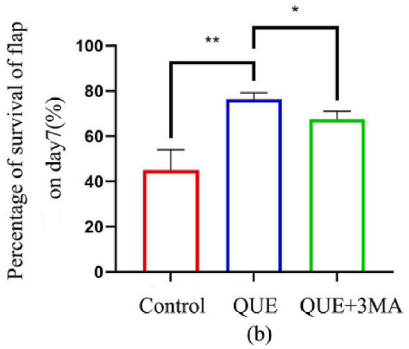

(b)

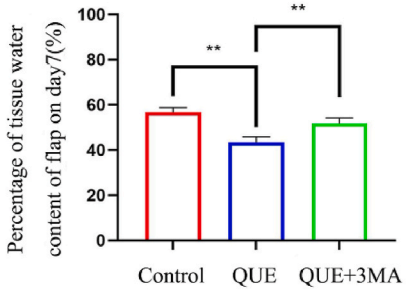

(d)

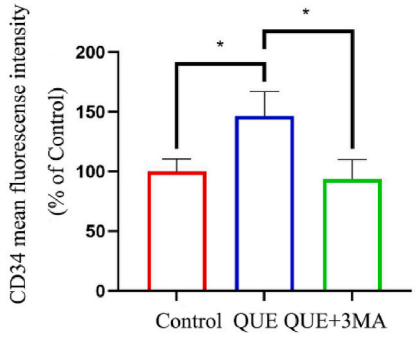

(f)

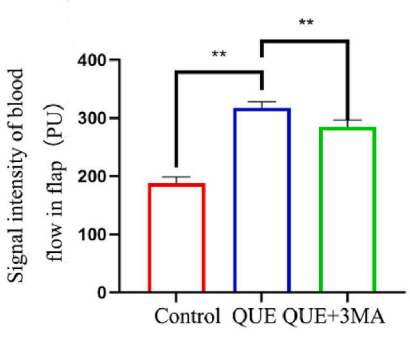

(h)

(caption on next page)

Fig. 3. |QUE could effectively enhance the random flap survival. (a) Photographs of the flap modeling area and visual images before and after vascular occlusion. (b) Photographs of flap survival area. (c) Photographs of flap edema area. (d) Chart of the percentage of the skin flap stock area in each group for 7 days. (e) Chart of the percentage of the skin flap edema area in each group for 7 days. (f) Statistical result of blood flow signal intensity at 0 days, 3 days and 7days. (g) LDBF technique reveals the subcutaneous blood flow status at 0, 3, and 7 days post-operation. (h) H and E staining images of the control and QUE groups. Magnification was × 10, Scale bar 200 μm. (i) Masson's trichrome stain images of each group showing blood vessels and collagen fibers. Magnification: 10×; Scale bar 200 μm. (j) Mean vessel density. (k) Positive collagen fiber area. Data were expressed as mean ± SD, n = 3. "*"and"**"represent $p < 0.05$ or $p < 0.01$ versus the QUE group, indicating statistical significance.

Japan). Percentages of C-CASP3-positive cells, LC3II-positive cells, P62-positive cells, and CD34-positive microvessels were computed for six randomly selected fields from each tissue sample.

2.14. Statistical analysis

The Student's t-test was performed to compare the data obtained from two distinct groups in the experiment. Analysis of variance (ANOVA) and Tukey's post hoc analyses are commonly used in the statistical analysis of experiments involving more than two groups, as they allow for comprehensive data comparisons. Statistical analyses were conducted using software applications such as Excel and GraphPad Prism 7. The data were presented in the form of the mean ± standard deviation (SD). In this study, a p-value below the threshold of 0.05 was indicative of a statistically significant difference.

3. Results

3.1. QUE enhanced the proliferation and migration of HUVECs following oxidative stress injury

Angiogenesis is a key factor in promoting the survival of random flaps. Firstly, the CCK8 assay was utilized to quantify the biotoxicity of QUE. The results showed that the proliferative effect of QUE on HUVECs was enhanced with increasing concentration of QUE (Fig. 1a). Moreover, wound healing and transwell assays were carried out to assess the impact of QUE on the migration ability of HUVECs following oxidative damage. A notable reduction in the migration ability of HUVECs was observed following exposure to H_2O_2. However, this impaired migration ability was restored upon treatment with QUE (Fig. 1b–d). Then, BrdU was used to determine whether QUE could promote the proliferation of HUVECs following oxidative injury. The results indicated a significant decrease in the proliferation capacity of HUVECs upon exposure to H_2O_2, whereas the proliferation ability of HUVECs was significantly restored by QUE treatment (Fig. 1c–e). Crystal violet was used to label cells for the transwell migration assay, revealing that QUE could significantly improve the migration activity of cells stimulated by H_2O_2, which could be inhibited by the autophagy inhibitor 3 MA (Fig. 1f–g). In conclusion, QUE effectively restored the proliferation and migration ability of HUVECs after oxidative damage.

3.2. Systemic administration of QUE does not cause significant toxic damage

In order to assess the safety of systemic administration of QUE, the parenchymal organs were observed for lesions. H&E staining of the liver, kidney, and brain displayed no significant variations in the tissue structure and cell distribution after systemic administration of QUE (Fig. 2 a). Blood biochemical results showed that the CRE, ALT, and AST levels in the Control group and QUE group were within the normal range (Fig. 2b). In conclusion, systemic administration of QUE was deemed safe for the treatment of flaps.

3.3. QUE could effectively enhance the random flap survival

Furthermore, a mouse random flap model was constructed to verify the protective effect of QUE on random flaps (Fig. 3 a). From the apparent observation and edema of the mouse flap, QUE treatment was found to significantly inhibit distal necrosis of the mouse random flap (Fig. 3b–e). The Doppler results indicated no statistically significant disparity in blood perfusion between the control group and the QUE group at 0 and 3 days post-modeling. However, at 7 days post-modeling, significantly higher blood perfusion was observed in the QUE group compared to the control group (Fig. 3f–g). In addition, H&E staining demonstrated that QUE could significantly promote neovascularization, and Masson staining revealed that QUE promoted the ordering of collagen arrangement in flaps (Fig. 3h–k). In conclusion, QUE exerted a significant positive effect on the survival of random flaps.

3.4. Inhibition of autophagosome formation after QUE administration resulted in a decrease in the survival of random flaps

The distal part of the random flap is often in a state of nutrient deficiency, and autophagy acts as a defense mechanism to cope with energy shortage. After inhibiting autophagosome formation with 3 MA, the protection range of the QUE skin flap was significantly reduced and the tissue water content was increased (Fig. 4a–d). The CD34 immunofluorescence staining assay and the laser Doppler data revealed significantly increased neovasculature and blood perfusion in the QUE+3 MA group compared with the QUE group (Fig. 4e–h). H&E staining showed that the protective effect of QUE on tissue structure was weakened after 3 MA treatment, and the number of blood vessels per unit area was also significantly reduced (Fig. 4i–j). In addition, the WB results revealed that VEGF and MMP9, which promote angiogenesis, and the neovascular index CD34 were significantly increased after QUE treatment. In contrast, these indexes were significantly inhibited after 3 MA treatment (Fig. 4k–n). In conclusion, 3 MA significantly inhibited the therapeutic

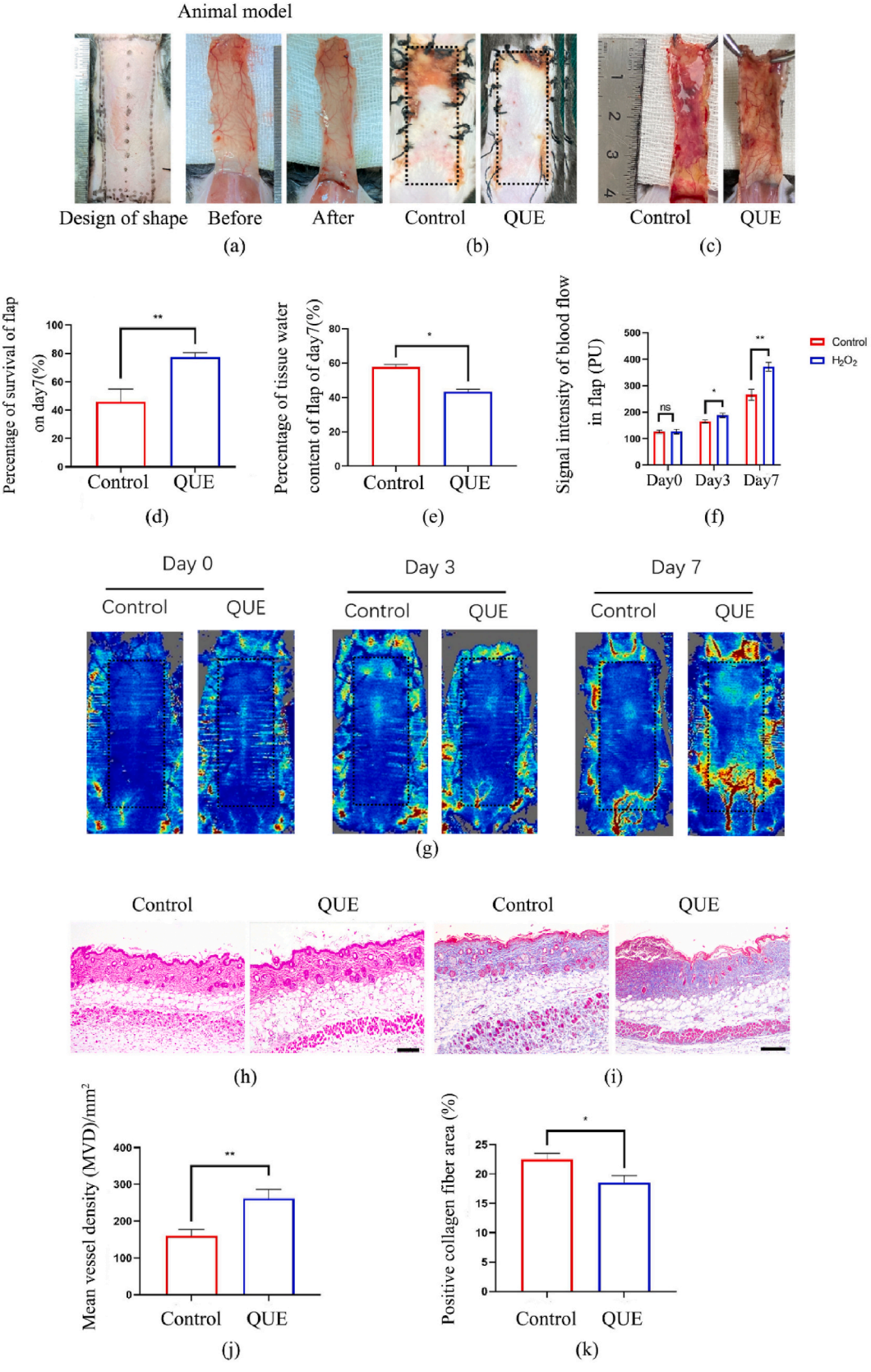
Animal model
Design of shape
Before
After
Control
QUE
Control
QUE
(a)
(b)
(c)
Percentage of survival of flap on day7(%)
Control
QUE
(d)
Percentage of tissue water content of flap of day7(%)
Control
QUE
(e)
Signal intensity of blood flow in flap (PU)
Day0
Day3
Day7
Control
H2O2
(f)
Day 0
Day 3
Day 7
Control
QUE
(g)
Control
QUE
Control
QUE
(h)
(i)
Mean vessel density (MVD)/mm2
Control
QUE
(j)
Positive collagen fiber area (%)
Control
QUE
(k)

Fig. 4. |Inhibition of autophagosome formation after QUE administration resulted in a decrease in the survival of random flaps. (a) Images reflecting flap survival at the seventh day after operation in the control group, treatment group with QUE, and treatment group with QUE+3 MA. (b) percentage of survival of flap on 7 day. (c) Images reflecting flap edema at the seventh day after operation in the control group, treatment group with QUE, and treatment group with QUE+3 MA. (d) Percentage of tissue water content of flap on 7 day. (e) Immunofluorescence showing the expression of CD34 (green), and DAPI (blue) in different groups. Magnification: 20×; Scale: 100 μm. (f) Mean fluorescence intensity of CD34 in different groups. (g) LDBF technique reveals the subcutaneous blood flow status at 7 days post-operation. (h) Statistical result of blood flow signal intensity at the seventh day. Scale: 0.5 cm. (i) H and E staining images of the control, QUE and QUE+3 MA groups. Magnification was × 10, Scale bar 400 μm. (j) Mean vessel density. (k) Western blot results showing the expression of VEGF, CD34 and MMP9 in different groups. (l–n) Quantitative analysis of VEGF, CD34 and MMP9 protein expressions. Data were expressed as mean ± SD, n = 3. "*"and"**"represent $p < 0.05$ or $p < 0.01$ versus the NT group, indicating statistical significance.

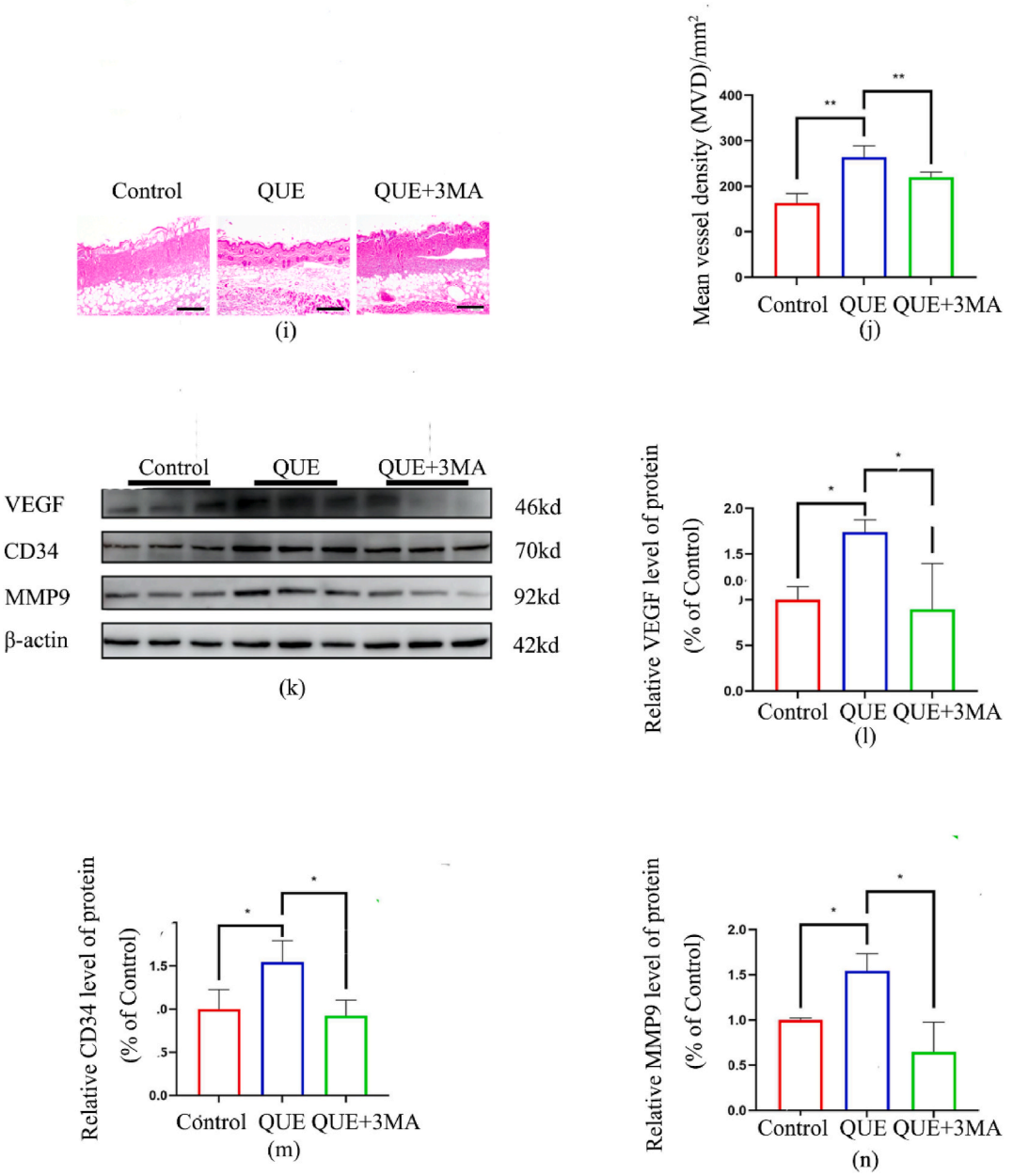

Fig. 4. (*continued*).

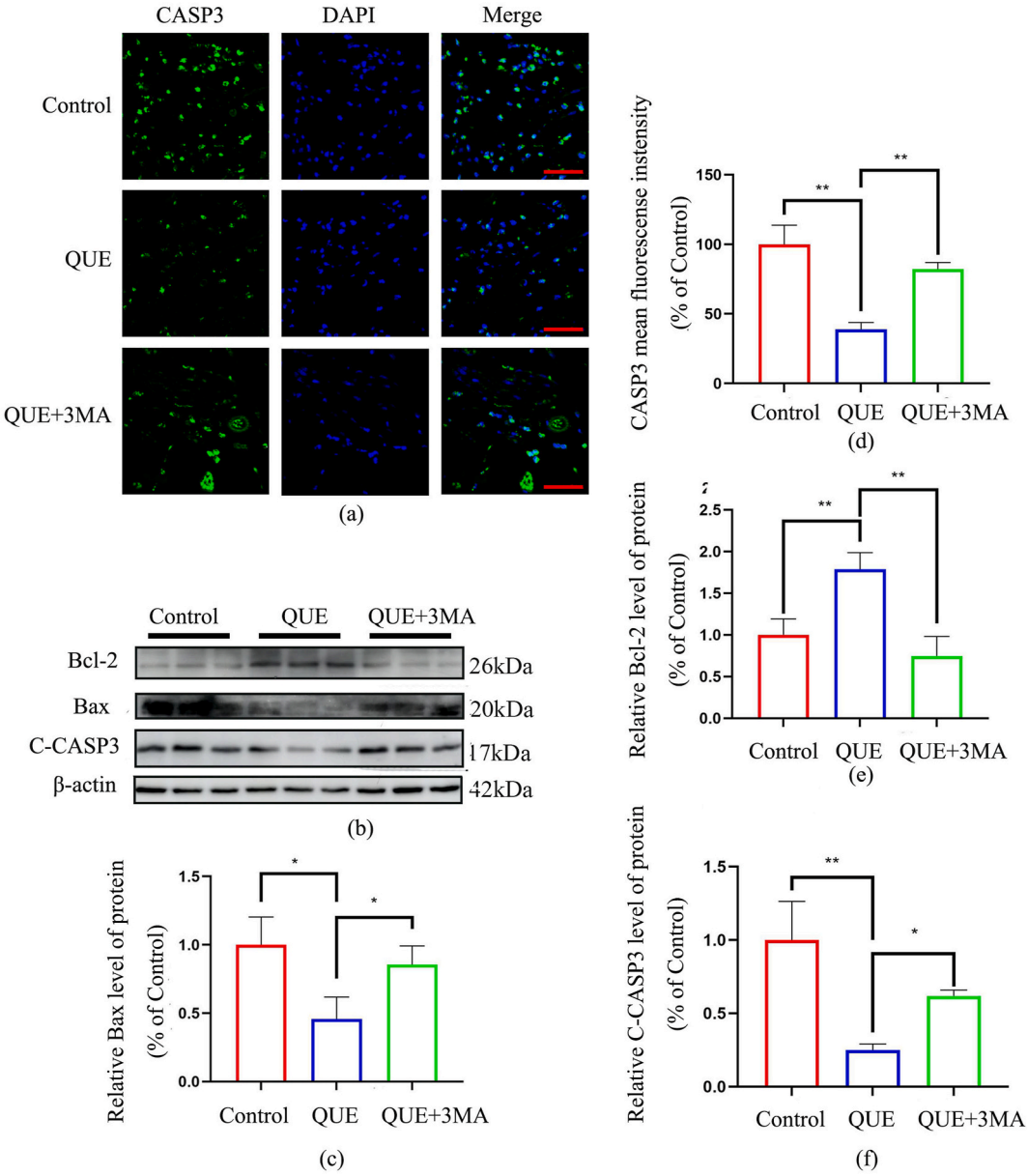

Fig. 5. |Inhibition of autophagosome formation after QUE administration resulted in increased apoptosis levels of the random flap. (a) Immunofluorescence showing the expression of CASP3 (green), and DAPI(blue) in different groups. Magnification: 20×; Scale: 200 μm. (b) Western blot results showing the expression of Bcl-2, Bax and C-CASP3 in different groups. (c) Quantitative analysis of Bax protein expressions. (d) Mean fluorescence intensity of CASP3 in different groups. (e) Quantitative analysis of Bcl-2 protein expressions. (f) Quantitative analysis of C-CASP3 protein expressions. Data were expressed as mean ± SD, n = 3. "*"and"**"represent $p < 0.05$ or $p < 0.01$ versus the NT group, indicating statistical significance.

effect of QUE, resulting in decreased survival of random flaps.

3.5. Inhibition of autophagosome formation after QUE administration resulted in increased apoptosis levels of the random flap

Furthermore, the apoptosis level of random flaps was detected. The immunofluorescence results indicated elevated apoptosis levels at the distal section of the random flaps. However, the apoptosis level was significantly reduced by QUE treatment, and the anti-apoptosis effect of QUE was significantly weakened after 3 MA treatment (Fig. 5a–d). The WB results indicated a significantly increased expression of apoptosis-inhibiting protein Bcl-2 after QUE treatment, while the expression of apoptosis-promoting proteins C-caspase3 and BAX was significantly decreased. After 3 MA treatment, QUE-inhibited apoptosis showed a rebound; the Bcl-2

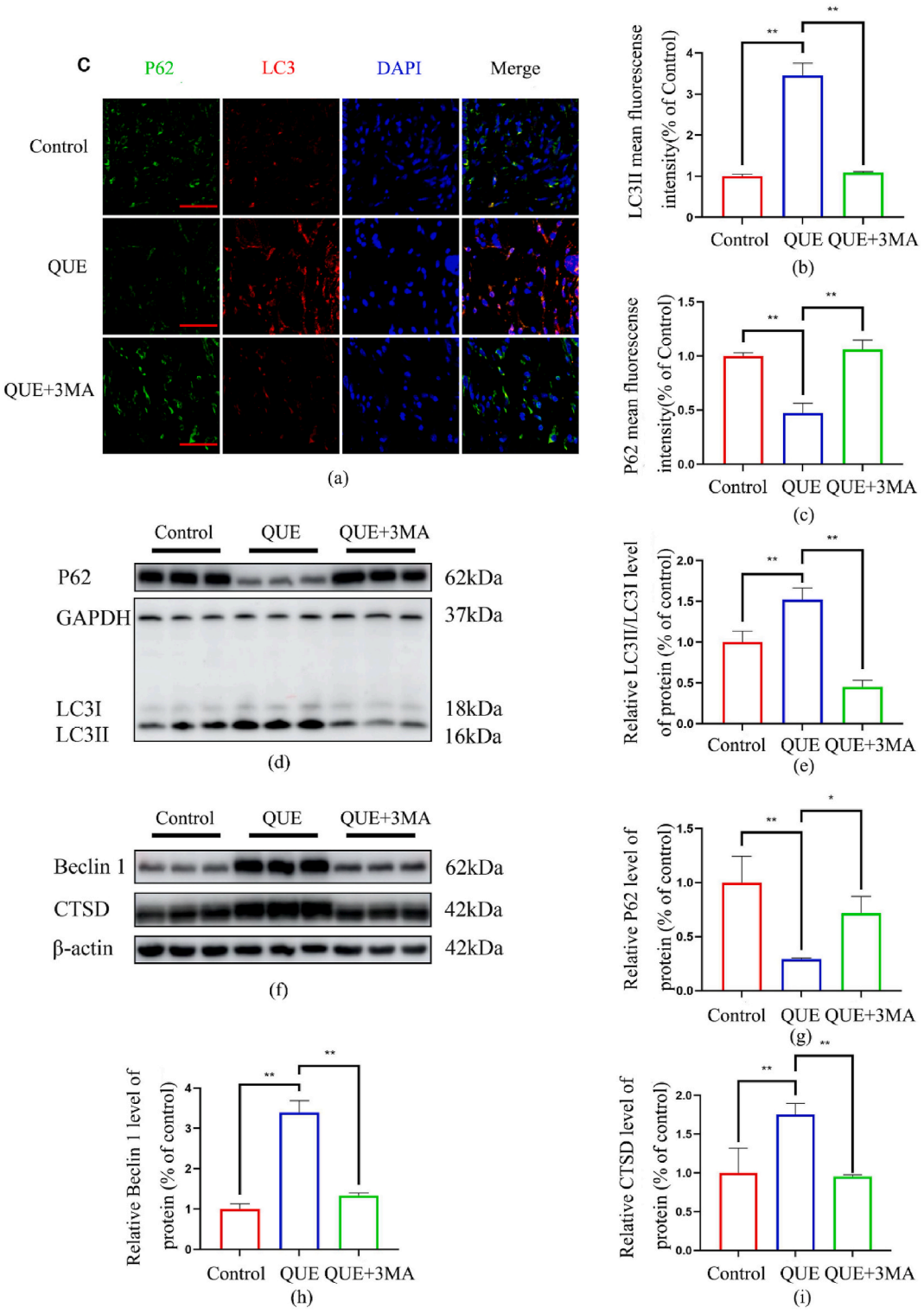

Fig. 6. |Activation of the autophagy pathway is a key pathway for QUE to enhance the survival of random flaps. (a) Immunofluorescence showing the expression of P62 (green), LC3(red) and DAPI(blue) in different groups. Magnification: 20×; Scale: 200 μm. (b,c) Mean fluorescence intensity of P62 and LC3 in different groups. (d) Western blot results showing the expression of P62 and LC3 in different groups. (e) Quantitative analysis of LC3 protein expressions.(f) Western blot results showing the expression of Beclin 1 and CTSD in different groups.(g) Quantitative analysis of P62 protein expressions. (h,i) Quantitative analysis of Beclin 1 and CTSD protein expressions. (j) Western blot results showing the expression of p-

AMPK, AMPK, P62 and LC3 in different groups. (k,l,m) Mean fluorescence intensity of p-AMPK/AMPK, P62 and LC3 in different groups. Data were expressed as mean ± SD, n = 3. "*"and "**" represent $p < 0.05$ or $p < 0.01$ versus the NT group, indicating statistical significance.

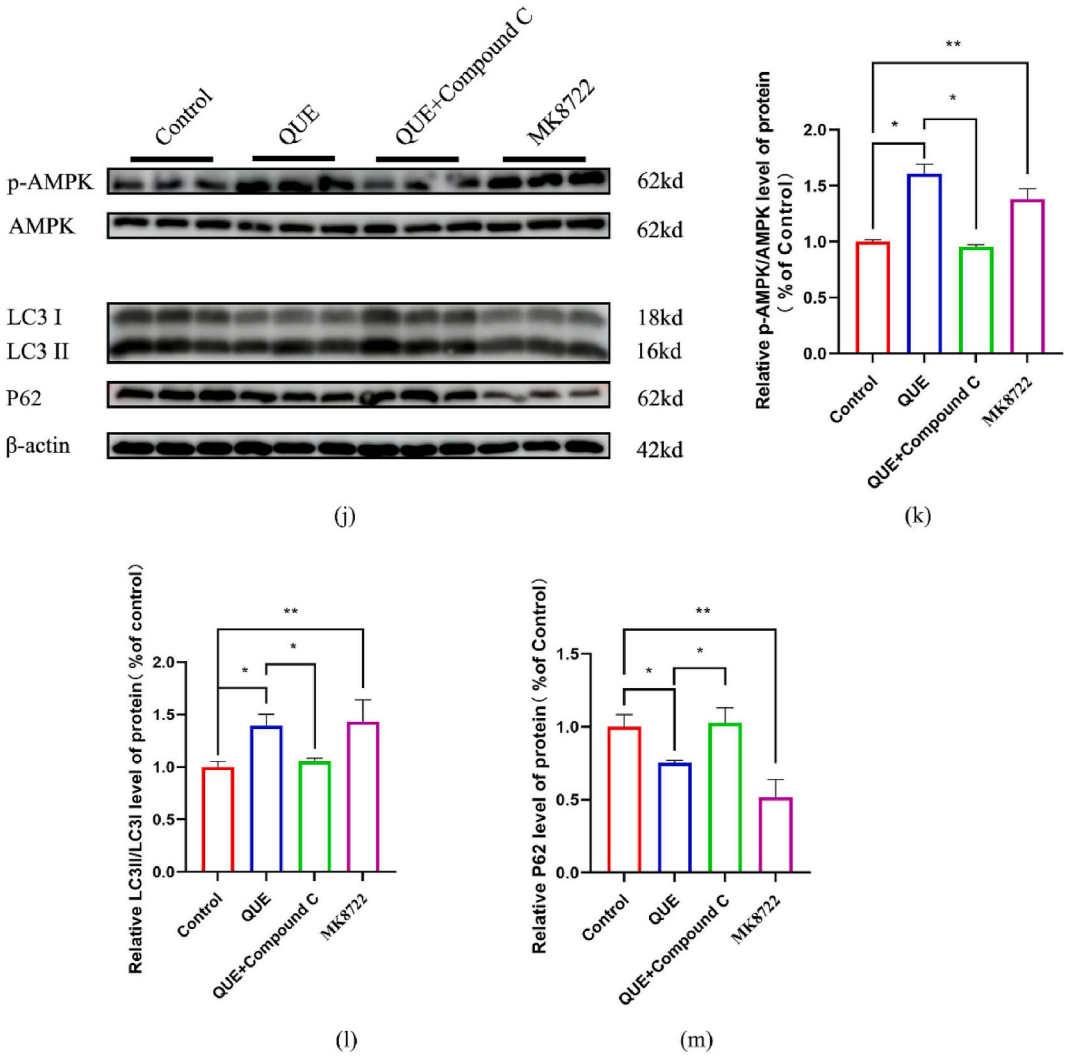

Fig. 6. (*continued*).

expression was inhibited and the expression of C-caspase3 and BAX increased (Fig. 4 b–c, e-f). In conclusion, inhibition of autophagosome formation by 3 MA decreases the inhibitory effects of QUE on apoptosis.

3.6. Activation of the autophagy pathway is a key pathway for QUE to enhance the survival of random flaps

Autophagy plays a significant role in QUE efficacy, but its specific pathway remains unclear. 3 MA inhibits autophagy by inhibiting class III PI3K, which is closely related to Beclin1 expression. In this study, the expression of autophagy and the effects of QUE on autophagy were evaluated by immunofluorescence and WB. The experimental results showed that autophagy was activated, and the flow of autophagy remained smooth after QUE treatment. However, autophagy activated by QUE was significantly inhibited after 3 MA (Fig. 6a–e). Subsequently, the role of Beclin1 in QUE-activated autophagy was determined. The WB results demonstrated that Beclin1 was significantly activated after QUE treatment and was accompanied by improved lysosome function. In contrast, Beclin expression was inhibited after 3 MA treatment, and lysosome function was reduced (Fig. 5f–i). Next, we examined the effect of activation of AMPK, a classical energy-promoting pathway, on the expression of AMPK and autophagy in the Control group, QUE group, QUE + Compound C group and MK8722 group. The results show that QUE can effectively activate AMPK phosphorylation and stimulate autophagy, which is consistent with the effect of AMPK activator MK8722. The autophagy effect in the QUE + Compound C group was significantly weakened after AMPK was inhibited by Compound C to suppress the activation of AMPK by QUE. In conclusion, improvement of energy metabolism by activation of autophagy by QUE is a key target for promoting random flap survival.

4. Discussion

Necrosis remains a relatively common negative outcome of random skin flaps due to distal ischemia [41,42]. In previous studies, vasoregenerative drugs were explored as first-choice treatments [43,44]. However, ischemia-reperfusion injury is a key factor limiting skin flap survival [45]. Therefore, this study focused on improving the adaptability of remote cells in random flaps to nutrient deficiency and the microenvironment.

Quercetin is widely found in angiosperms. It is an aglycone, which is often combined with sugar in the form of glycosides and has antioxidant and vascular protection functions [46–48]. In our study, systemic administration of QUE was found to improve the survival of randomized flaps without significant toxicity. Hence, this study discussed and analyzed the targets of quercetin.

Autophagy refers to the process of using lysosomes to degrade and reuse damaged, denatured, misfolded, or senescent macromolecules (proteins) and damaged organelles through intracellular pathways [49]. Under pathological conditions, autophagy is often activated as a cellular protective mechanism to maintain the overall balance [50]. The inhibition of autophagy in the distal ischemic necrotic area of random flaps has been widely reported [51,52]. Activating autophagy is a key mechanism to reduce the distal ischemic necrosis of random flaps. In our study, quercetin was found to effectively activate autophagy and inhibit apoptosis in the distal ischemic region of random flaps. Beclin1 is a key target in the autophagy pathway, and studies have shown that the expression of Beclin1 and Bcl-2 is parallel. In addition, Bcl-2 expression was down-regulated after treatment with the autophagy inhibitor 3 MA; thus, experiments were carried out to determine whether Beclin1 was upstream of autophagy. Furthermore, WB showed a significant upregulation in Beclin1 expression protein following QUE treatment. Treatment with the autophagy inhibitor 3 MA significantly inhibited QUE-induced autophagy, accompanied by a significant down-regulation of Beclin1. Meanwhile, we detected the activation of the energy metabolism pathway AMPK by QUE, and set up a inhibition group and positive control group by using agonists and inhibitors simultaneously for comparative analysis. We concluded that QUE activates autophagy while effectively improving energy metabolism in the distal ischemic area of random flaps, which is one of the key mechanisms by which QUE promotes the survival of random flaps.

In conclusion, QUE can improve cell tolerance in the distal ischemic region of random flaps by activating autophagy, which can resist the complex and variable microenvironment and improve the survival of random flaps.

Data availability statement

The data used to support the findings of this study are available from the corresponding author upon request.

CRediT authorship contribution statement

Xin Zheng: Investigation, Data curation. **Yiyu Wang:** Writing – review & editing, Software, Methodology, Formal analysis. **Xiaokang Gong:** Writing – review & editing, Software, Project administration, Funding acquisition, Data curation. **Weijie Chen:** Writing – original draft, Methodology, Data curation. **Wenbiao Zheng:** Writing – review & editing, Project administration, Formal analysis, Conceptualization. **Tao Chen:** Writing – original draft, Formal analysis, Data curation, Conceptualization.

Declaration of competing interest

All authors declare no conflict of interest.

Acknowledgments

This study was partly funded by a grant the Zhejiang Provincial Natural Science Foundation of China(LTGD23H060001), the Medical Health Science and Technology Project of Zhejiang Provincial Health Commission (2022RC084), the Traditional Chinese Medicine Science and Technology Project of Zhejiang Provincial Health Commission(2023ZL774)and the Science and Technology Program of Taizhou (23ywb63).

References

[1] H.P. Gaboriau, C.S. Murakami, Skin anatomy and flap physiology, Otolaryng Clin N Am 34 (3) (2001) 555.
[2] A. Costeloe, J. Newman, Aesthetician role in facial plastic surgery and systemic therapy for healthy skin, Facial Plast Surg Cl 31 (4) (2023) 557–566.
[3] H. Hyakusoku, J.H. Gao, D.G. Pennington, R. Aoki, M. Murakami, R. Ogawa, The microvascular augmented subdermal vascular network (ma-SVN) flap: its variations and recent development in using intercostal perforators, Brit J Plast Surg 55 (5) (2002) 402–411.
[4] T.H. Park, The utility of hyaluronidase for the free and pedicle flap salvage, J. Craniofac. Surg. 34 (3) (2023) 1058–1060.
[5] L.J. Wu, S.Y. Gao, K. Tian, T.L. Zhao, K. Li, "Pingpong racket" flap model for evaluating flap survival, J Cosmet Dermatol-Us 20 (8) (2021) 2593–2597.
[6] Y.H. Wang, Y. Mi, J.H. Tian, X. Qiao, X.L. Su, J. Kang, Z.J. Wu, G.Q. Wang, X.S. Zhou, Y. Zhou, R.S. Li, Intermedin alleviates renal ischemia-reperfusion injury and enhances neovascularization in wistar rats, Drug Des. Dev. Ther. 14 (2020) 4825–4834.
[7] J.B. He, X.Y. Ma, W.J. Li, Y.Y. Liu, D.S. Lin, Exenatide inhibits necrosis by enhancing angiogenesis and ameliorating ischemia/reperfusion injury in a random skin flap rat model, Int Immunopharmacol 90 (2021).
[8] H. Cui, Y.Y. Feng, C.L. Shu, R.T. Yuan, L.X. Bu, M.Y. Jia, B.X. Pang, Dietary nitrate protects against skin flap ischemia-reperfusion injury in rats modulation of antioxidative action and reduction of inflammatory responses, Front. Pharmacol. 10 (2020).
[9] S.X. Zhang, J.L. Tang, C. Sun, N.N. Zhang, X.Q. Ning, X.Q. Li, J.Q. Wang, Dexmedetomidine attenuates hepatic ischemia-reperfusion injury-induced apoptosis via reducing oxidative stress and endoplasmic reticulum stress, Int Immunopharmacol 117 (2023).

[10] K. Odake, M. Tsujii, T. Iino, K. Chiba, T. Kataoka, A. Sudo, Febuxostat treatment attenuates oxidative stress and inflammation due to ischemia-reperfusion injury through the necrotic pathway in skin flap of animal model, Free Radical Bio Med 177 (2021) 238–246.
[11] S.W. Ryter, D. Bhatia, M.E. Choi, Autophagy: a lysosome-dependent process with implications in cellular redox homeostasis and human disease, Antioxid Redox Sign 30 (1) (2019) 138–159.
[12] K.K. Mahapatra, S.R. Mishra, B.P. Behera, S. Patil, D.A. Gewirtz, S.K. Bhutia, The lysosome as an imperative regulator of autophagy and cell death, Cell. Mol. Life Sci. 78 (23) (2021) 7435–7449.
[13] W.W.Y. Yim, N. Mizushima, Lysosome biology in autophagy, Cell Discov 6 (1) (2020).
[14] L. Yu, Y. Chen, S.A. Tooze, Autophagy pathway: cellular and molecular mechanisms, Autophagy 14 (2) (2018) 207–215.
[15] V. Guhe, B. Soni, P. Ingale, S. Singh, Autophagy proteins and its homeostasis in cellular environment, Adv Protein Chem Str 123 (2021) 73–93.
[16] S.Y. Cheon, H. Kim, D.C. Rubinsztein, J.E. Lee, Autophagy, cellular aging and age-related human diseases, Exp Neurobiol 28 (6) (2019) 643–657.
[17] J.S. Lou, H.J. Zhang, J.J. Qi, Y. Xu, X.Y. Wang, J.T. Jiang, X.L. Hu, L.B. Ni, Y.P.A. Cai, X.Y. Wang, W.Y. Gao, J. Xiao, K.L. Zhou, Cyclic helix B peptide promotes random-pattern skin flap survival via TFE3-mediated enhancement of autophagy and reduction of ROS levels, Brit J Pharmacol 179 (2) (2022) 301–321.
[18] N.N. Yang, G.X. Yu, Y.Y. Lai, J.Y. Zhao, Z.L. Chen, L. Chen, Y.D. Fu, P. Fang, W.Y. Gao, Y.P. Cai, Z.J. Li, J. Xiao, K.L. Zhou, J. Ding, A snake cathelicidin enhances transcription factor EB-mediated autophagy and alleviates ROS-induced pyroptosis after ischaemia-reperfusion injury of island skin flaps, Brit J Pharmacol (2023).
[19] M.L. Bi, Y.H. Qin, L.T. Zhao, X.F. Zhang, Edaravone promotes viability of random skin flaps via activating PI3K/Akt/mTOR signalling pathway-mediated enhancement of autophagy, Int. Wound J. 20 (8) (2023) 3088–3104.
[20] H.T. Ye, F.D. Li, Y. Shen, X.Z. Wu, L. Zhao, H.J. Zhang, J.X. Yang, X.L. Shui, Rosuvastatin promotes survival of random skin flaps through AMPK-mTOR pathway-induced autophagy, Int Immunopharmacol 118 (2023).
[21] B.L. Li, Z.T. Chen, X.B. Luo, C.X. Zhang, H.Y. Chen, S.X. Wang, M.Y. Zhao, H.W. Ma, J.L. Liu, M.S. Cheng, Y.Y. Yang, H.D. Yan, Butylphthalide inhibits autophagy and promotes multiterritory perforator flap survival, Front. Pharmacol. 11 (2021).
[22] F.F. Chen, J.Y. Zhan, X.Q. Yan, A. Al Mamun, Y. Zhang, Y.T. Xu, H.Y. Zhang, X.K. Li, K.L. Zhou, J. Xiao, FGF21 alleviates microvascular damage following limb ischemia/reperfusion injury by TFEB-mediated autophagy enhancement and anti-oxidative response, Signal Transduct Tar 7 (1) (2022).
[23] B. Mathew, M. Chennakesavalu, M. Sharma, L.A. Torres, C.R. Stelman, S. Tran, R. Patel, N. Burg, M. Salkovski, K. Kadzielawa, F. Seiler, L.N. Aldrich, S. Roth, Autophagy and post-ischemic conditioning in retinal ischemia, Autophagy 17 (6) (2021) 1479–1499.
[24] D.M. Zhang, T. Zhang, M.M. Wang, X.X. Wang, Y.Y. Qin, J.C. Wu, R. Han, R. Sheng, Y. Wang, Z. Chen, F. Han, Y.Q. Ding, M. Li, Z.H. Qin, TIGAR alleviates ischemia/reperfusion-induced autophagy and ischemic brain injury, Free Radical Bio Med 137 (2019) 13–23.
[25] S.V. Popov, A. Mukhomedzyanov, N.S. Voronkov, I.A. Derkachev, A.A. Boshchenko, F. Fu, G.Z. Sufianova, M.S. Khlestkina, L.N. Maslov, Regulation of autophagy of the heart in ischemia and reperfusion, Apoptosis 28 (1–2) (2023) 55–80.
[26] D.F. Lou, X.Y. Xing, Y.Y. Liang, Dendrobine modulates autophagy to alleviate ox-LDL-induced oxidative stress and senescence in HUVECs, Drug Develop Res 83 (5) (2022) 1125–1137.
[27] L. Zhou, Y.L. Han, Q.J. Yang, B. Xin, M.Y. Chi, Y. Huo, C. Guo, X.P. Sun, Scutellarin attenuates doxorubicin-induced oxidative stress, DNA damage, mitochondrial dysfunction, apoptosis and autophagy in H9c2 cells, cardiac fibroblasts and HUVECs, Toxicol. Vitro 82 (2022).
[28] X.M. Yan, X.Y. Shang, Z.Q. Feng, B.Y. Chen, Y.R. Wu, Y. Zhou, Y. Li, L. Zhang, Triterpenoid saponins of Ilex pubescens against TNF-α induced inflammation and apoptosis in human umbilical vein endothelial cells via autophagy pathway, J. Pharm. Pharmacol. 74 (12) (2022) 1749–1757.
[29] F. Aghababaei, M. Hadidi, Recent advances in potential health benefits of quercetin, Pharmaceuticals-Base 16 (7) (2023).
[30] F.R. Mansour, I.A. Abdallah, A. Bedair, M. Hamed, Analytical methods for the determination of quercetin and quercetin glycosides in pharmaceuticals and biological samples, Crit. Rev. Anal. Chem. (2023).
[31] G.Z. Wang, Y.H. Wang, L.L. Yao, W. Gu, S.C. Zhao, Z.Y. Shen, Z.H. Lin, W. Liu, T.D. Yan, Pharmacological activity of quercetin: an updated review, Evid-Based Compl Alt 2022 (2022).
[32] W.W. Zhang, Y. Zheng, F. Yan, M.Q. Dong, Y.Z. Ren, Research progress of quercetin in cardiovascular disease, Front Cardiovasc Med 10 (2023).
[33] J. Li, J.N. Wang, Z.Q. Huang, X.D. Cui, C. Li, Oxidized quercetin has stronger anti-amyloid activity and anti-aging effect than native form, Comp Biochem Phys C 271 (2023).
[34] S. Mousavi, S. Vakili, F. Zal, A. Savardashtaki, M. Jafarinia, S. Sabetian, D. Razmjoue, A. Veisi, O. Azadbakht, M. Sabaghan, H. Behrouj, Quercetin potentiates the anti-osteoporotic effects of alendronate through modulation of autophagy and apoptosis mechanisms in ovariectomy-induced bone loss rat model, Mol. Biol. Rep. 50 (4) (2023) 3693–3703.
[35] M. Dogan, Assessment of mechanism involved in the apoptotic and anti-cancer activity of Quercetin and Quercetin-loaded chitosan nanoparticles, Med. Oncol. 39 (11) (2022).
[36] T.T. Wang, X.C. Feng, L.Z. Li, J. Luo, X.B. Liu, J. Zheng, X.J. Fan, Y.P. Liu, X.L. Xu, G.H. Zhou, L. Chen, Effects of quercetin on tenderness, apoptotic and autophagy signalling in chickens during post-mortem ageing, Food Chem. 383 (2022).
[37] R. Li, L. Chen, G.M. Yao, H.L. Yan, L. Wang, Effects of quercetin on diabetic retinopathy and its association with NLRP3 inflammasome and autophagy, Int J Ophthalmol-Chi 14 (1) (2021) 42–49.
[38] Y.Y. Wang, M. Xiong, M.S. Wang, H.D. Chen, W.J. Li, X.Z. Zhou, Quercetin promotes locomotor function recovery and axonal regeneration through induction of autophagy after spinal cord injury, Clin Exp Pharmacol P 48 (12) (2021) 1642–1652.
[39] A.W. Filho, V.C. Filho, L. Olinger, M.M. de Souza, Quercetin: further investigation of its antinociceptive properties and mechanisms of action, Arch Pharm. Res. (Seoul) 31 (6) (2008) 713–721.
[40] C. Dong, Z. Chen, L. Zhu, N. Bsoul, H. Wu, J. Jiang, X. Chen, Y. Lai, G. Yu, Y. Gu, X. Guo, W. Gao, Diallyl trisulfide enhances the survival of multiterritory perforator skin flaps, Front. Pharmacol. 13 (2022) 809034.
[41] J.S. Lou, X.Y. Wang, H.J. Zhang, G.X. Yu, J. Ding, X.W. Zhu, Y. Li, Y.S. Wu, H. Xu, H.Z. Xu, W.Y. Gao, J. Xiao, K.L. Zhou, Inhibition of PLA2G4E/cPLA2 promotes survival of random skin flaps by alleviating Lysosomal membrane permeabilization-Induced necroptosis, Autophagy 18 (8) (2022) 1841–1863.
[42] H.Q. Wu, J. Ding, S.H. Li, J.T. Lin, R.H. Jiang, C. Lin, L. Dai, C.L. Xie, D.S. Lin, H.Z. Xu, W.Y. Gao, K.L. Zhou, Metformin promotes the survival of random-pattern skin flaps by inducing autophagy via the AMPK-mTOR-TFEB signaling pathway, Int. J. Biol. Sci. 15 (2) (2019) 325–340.
[43] K. Gideroglu, S. Alagoz, F. Uygur, R. Evinc, B. Celikoz, G. Bugdayci, Effects of nebivolol on skin flap survival: a randomized experimental study in rats, Curr Ther Res Clin E 69 (5) (2008) 449–458.
[44] K. Hart, D. Baur, J. Hodam, L. Lesoon-Wood, M. Parham, K. Keith, R. Vazquez, E. Ager, J. Pizarro, Short- and long-term effects of sildenafil on skin flap survival in rats, Laryngoscope 116 (4) (2006) 522–528.
[45] Z.M. Yin, H.W. Ren, L.Q. Liu, W.L. Chen, C. Gan, H. Jiao, J.C. Fan, Thioredoxin protects skin flaps from ischemia-reperfusion injury: a novel prognostic and therapeutic target, Plast. Reconstr. Surg. 137 (2) (2016) 511–521.
[46] T. Hatahet, M. Morille, A. Shamseddin, A. Aubert-Pouëssel, J.M. Devoisselle, S. Bégu, Dermal quercetin lipid nanocapsules: influence of the formulation on antioxidant activity and cellular protection against hydrogen peroxide, Int J Pharmaceut 518 (1–2) (2017) 167–176.
[47] Y. Gui, K. Qin, Y. Zhang, X.Y. Bian, Z.G. Wang, D.A.P. Han, Y. Peng, H.Y. Yan, Z.X. Gao, Quercetin improves rapid endothelialization and inflammatory microenvironment in electrospun vascular grafts, Biomed Mater 17 (6) (2022).
[48] R. Rezaei-Sadabady, A. Eidi, N. Zarghami, A. Barzegar, Intracellular ROS protection efficiency and free radical-scavenging activity of quercetin and quercetin-encapsulated liposomes, Artif Cell Nanomed B 44 (1) (2016) 128–134.
[49] J.N.S. Vargas, M. Hamasaki, T. Kawabata, R.J. Youle, T. Yoshimori, The mechanisms and roles of selective autophagy in mammals, Nat Rev Mol Cell Bio 24 (3) (2023) 167–185.

[50] T. Kawabata, T. Yoshimori, Autophagosome biogenesis and human health, Cell Discov 6 (1) (2020).
[51] H.Q. Wu, H.W. Chen, Z.L. Zheng, J.F. Li, J. Ding, Z.H. Huang, C. Jia, Z.T. Shen, G.D. Bao, L.Y. Wu, A. Al Mamun, H.Z. Xu, W.Y. Gao, K.L. Zhou, Trehalose promotes the survival of random-pattern skin flaps by TFEB mediated autophagy enhancement, Cell Death Dis. 10 (2019).
[52] Z.Y. Huang, X.B. Luo, Y.F. Zhang, Y.B. Ying, X. Cai, W.J. Lu, J. Zhao, Y.T. Wang, W.W. Lin, Y.R. Tu, Z.Y. Xiang, Q.J. Wu, S.W. Yang, S.P. Zhu, X.Y. Li, Notoginseng triterpenes inhibited autophagy in random flaps the beclin-1/VPS34/LC3 signaling pathway to improve tissue survival, Front Bioeng Biotech 9 (2021).